

CHARACTERISTIC HELICOPTER FLIGHT MECHANICS AND MOTION CUEING INTEGRATION INTO THE SIVOR ROBOTIC FLIGHT SIMULATOR: AN OBJECTIVE APPROACH

Diego F. Hidalgo* , Guilherme B. Rodamilans** Wesley R. de Oliveira**

**Instituto Tecnológico de Aeronáutica ,

Praça Marechal Eduardo Gomes, 50, Vila das Acácias, São José dos Campos, São Paulo, Brasil CEP 12228-900

*Universidad Pontificia Bolivariana

Circular 1a 70-01, Medellín, Antioquia, Colombia

Keywords: *Flight Simulation Robotics Motion Cueing*

Abstract

*The following paper will depict the process followed to build a baseline motion cueing setting specific for VTOL and helicopter applications for the **SIVOR** flight simulator at ITA. This effort is built around three elements: a pilot model, an identified model of the robotic platform and a set of surrogate flight dynamic models representative of helicopter motion. Initially, a description of the platform and simulation environment is presented, followed by the tuning strategy based on numerical optimization and a test case which will serve as a validation for the optimization strategy. A brief description of the **SIVOR** system identification process is presented along with the structural-pilot-model used to explore a set of three main manoeuvres which are used for washout filter tuning. Optimization results included in the test maneuvers show good agreement with published experimental observations.*

1 Introduction and Background

As part of the effort of capabilities build-up for the Robotic-Motion platform for Flight Simulation at Instituto Tecnológico de Aeronáutica (ITA), or **SIVOR** for its portuguese acronym, a parallel effort to that for fixed wing flight simulation has been set to integrate the rotorcraft flight

simulation case.

To such end, this work shows the initial steps to achieve integration of rotorcraft and related VTOL flight mechanics. This is done taking advantage of a robotic motion platform and by considering characteristic flight mechanics of helicopters (such as vertical or coupled roll-sway motions), which are then integrated into the flight simulation system. Besides the particularities of the case under study, the approach to the simulation-pilot-motion loop problem remains typical, i.e., such that the accelerations perceived by the pilot match as best as possible those of actual flight and that the final command inputs and system response also match that of the actual system. The goal of this effort is, more specifically, to define and tune a set of washout filters to enable the robot to generate motion cues within the limitations of its dynamic range. To do so, the actual pilot is kept off the simulation loop, instead, a structural-pilot-model (SPM) using a vestibular model is used, such that it would provide a closer baseline tuning to that which would eventually be accepted by human pilots, hopefully diminishing the required time and complexity of the subjective evaluation stage. So exposed, this work is built as a model-based system development exercise, which depends on three model-components: The pilot-model, the robotic-motion-platform represented by an iden-

tified model and a set of surrogate models representing some of the characteristic flight mechanics of helicopters, being in this case, a bob-up, roll-sway and yaw manoeuvres. The reason behind the proposed approach lays upon the recommendations of the Garteur Action Group 12 (HC-AG12), see [1] and [2], where simulation fidelity is presented as the result of two main portions of fidelity build-up. First, the so-called *predictive fidelity* related to a *physical tuning* and the remaining portion, *perceived fidelity* linked to subjective tuning [3]. The predictive fidelity consideration is made more in regard to the flight mechanics and system models used in the simulation, and the subjective portion is related to the tuning modifications extracted from pilots opinions. As one of the general observations of the action group, a gap exists between both portions in regard to fidelity metrics. Thus, in this case, the a pilot model is included for motion cueing tuning, hoping to explore its function to contribute to fill the gap.

2 SIVOR Simulator

The *SIVOR* full-motion flight simulation system is built around, for this work, a Kuka™ KR-500 robotic arm with a fixed base, although it can also be switched to a Kuka™ TITAN robot with a translation rail. The system, is set such that it is able to be compatible with several sources of input data and integration of sub-systems, being operated through a LabView® interface parting from the governing robot model already existing specifically for SIVOR. Thus, the general system architecture allows pilot inputs and simulation to be run independently, respecting the constant 12ms robot execution time loop or "*heartbeat*". While the visual environment could run at the same frequency of 84Hz it is usually limited to 60Hz due to visuals hardware limitations. Simulation environment for the helicopter case consists of a coupling of Matlab® SimuLink® and FlightGear. The arrangement was set so that the Flight Mechanics models would be built and executed in SimuLink® serving as receiver for pilot commands and at the same time transmitting the

vehicle response to FlightGear to be visualized by the pilot in the cockpit. The FlightGear simulator was included only as a visuals generator, taking advantage of its flexible settings for communication and integration. While the architecture allows for full simulation, in this work, only motion cueing is considered, leaving the visual feedback as part of the Structural Pilot Model.



Fig. 1 SIVOR robot

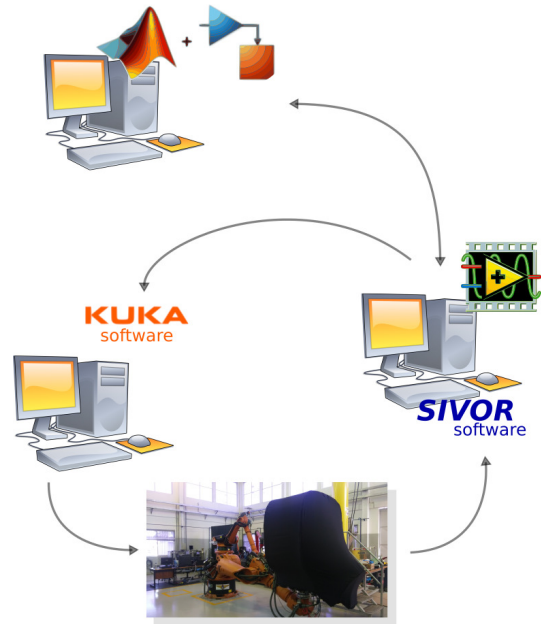


Fig. 2 SIVOR Integration

3 Models and considerations

This work follows that of Schroeder [4] for the special case of helicopter flight simulation requirements. In his report Schroeder proposed

the evaluation of motion cueing using a pilot model for a vertical relocation manoeuvre (bob-up), leading to think that the inclusion of a pilot model may be useful to address the interaction between pilot and simulation in regard to motion cueing and system tuning. Previous work have shown the inclusion of pilot models in other systems couplings, for instance, adverse Rotorcraft Pilot Coupling (RCP) phenomena has been explored (see [5]) and a series of active and passive pilot models have been used to address the issue. On the other hand, the body of work related to motion cueing for flight simulation included the contributions of several authors whom have added other aspects to increase the objectivity in regard to the whole simulation experience (see [8], [9],[10],[11],[12]). Since motion cueing is also subject to subjective influence, it is a variable matter dependent on pilot physiology, tending to generate unbalanced judgement even in the cases of highly trained individuals, an attempt to reduce the noise around the pilot acceptance is proposed by using a pilot model adjusted for every specific manoeuvre. The value of this approach follows that of other aircraft-pilot couplings which also included pilot models, assuming, for this case, that motion cueing is but one of several channels of aircraft-pilot coupling.

3.1 The pilot model

3.1.1 The Structural Pilot Model

While there exist a wide span of pilot models, for which the reader is referred, for instance to reviews like [7] and [5], covering from simple compensatory models, passing through passive and active models up to optimal control based approaches, it was considered that the Structural Pilot Model (SPM) provided enough flexibility with the adequate level of fidelity without the level of information required by more sophisticated models. Besides, Schroeder [4] used the SPM to evaluate one of the discrete manoeuvres used for his helicopter flight simulation requirements, thus providing an initial point for this study. The SPM developed by Hess [13] has also been used for flight simulation evaluations [14]

[15] [17] and provided insight in regard to corrections to improve simulation fidelity. A relevant assumption for this work is the combination of signals, visual and motion, within the pilot model structure. In [16] Hess and Siwakosit proposed a surrogate cue for a roll-sway maneuver. Structured around two closed control loops, the maneuver included the surrogate cue extracted from acceleration perception summed to the visual cue in the internal loop controlling the roll angle ϕ_{roll} and leaving the outer loop, controlling the lateral position y_{pos} as a visual cue only. As proposed by Hess and Siwakosit, the visual cue would represent a 75% of the total signal, and the perceived acceleration portion would add the remaining 25%. This assumption is kept in this work in order to capture the motion cues provided by the robotic platform. The general procedure for parameter selection for the SPM for this work follows that of refs. [13] and [18]

The corresponding SPM block model for this work is presented in Fig. 3.

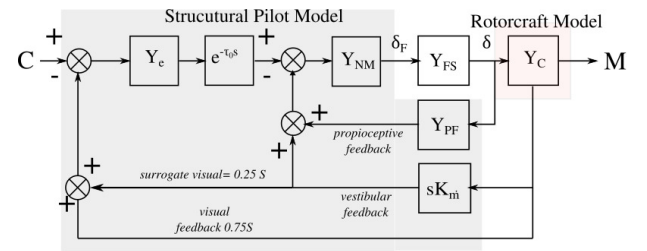


Fig. 3 Structural Pilot Model with surrogate visual cue modification (based on [18])

3.1.2 Vestibular system model

In this work, pilot perception of motion is represented by a vestibular model, in order to provide a point of observation of the net accelerations affecting the control loop. This, it is hoped, will provide a closer matching to pilots approval of the whole simulation system while reducing subjectivity.

The models used for this case correspond to two transfer functions representing the otolith and semi-circular channels. Thus the transfer functions correspond to [19]:

$$H_{oto} = \frac{0.4(13.2s + 1)}{(5.33s + 1)(0.66s + 1)} \quad (1)$$

for the Otolith, capturing linear forces and

$$H_{ssc} = \frac{456s^2}{(5.7s + 1)(80s + 1)} \quad (2)$$

for the Semi-circular channel capturing angular rates.

3.2 Motion Washout filters

To compensate for limitations in the robot's range of motion, a set of Washout Filters (WoF) is introduced to govern the different robot motions within the corresponding limits while allowing a better fit against actual acceleration perception. Following the Classic Washout Filter from Reid and Nahon [20], translational motion channels are treated with a second-order High-Pass filter (HPf) as shown

$$HP_{sim}^i = k \frac{s^2}{s^2 + 2\zeta_{hp_i}\omega_{hp_i}s + \omega_{hp_i}^2} \quad (3)$$

With $i : x, y, z$.

Angular rates $[p, q, r]$ treatment is done using also a second-order filter such that

$$HP_{sim}^\alpha = k \frac{s^2}{s^2 + 2\zeta_{hp_\alpha}\omega_{hp_\alpha}s + \omega_{hp_\alpha}^2} \quad (4)$$

with $\alpha : \phi, \theta, \psi$

3.3 Robot system identification

In this section, only a summary of the process followed for the robot system identification is presented, a future reference from the authors of this paper will be committed to a more detailed description in this regard.

The black-box time-domain parametric identification approach is applied, since the input/output data from the closed-loop system is available from the KUKA RSI controller with a 12 ms heartbeat, but a prior model structure is unknown [21]. Notwithstanding, considering the

previous approaches from Teufel [22], and that the classical purpose for a controlled robot is to bring it to a linear external behavior [23].

When using the KUKA Robotic System (manipulator + RSI controller) there may be some additional path calculator blocks for the cartesian-space approach. Besides that, as previously demonstrated by Teufel et.al. [22], the system always will present a transport-delay (e^{-Ts} and a discrete moving average filter on the input. Considering the empirical perceived decoupling among the six d.o.f. of the robotic system the multivariable approach is reduced to six independent channels for each d.o.f. of the robot. Primarily, the inner transfer functions blocks for each channel of the multivariable robotic system are approximated as traditional single-input-single-output (SISO) time-invariant linear second-order systems, $G_i(s)$, so that the parametric approach could be further understood in terms of the classical closed-loop performance indicators: damping (ζ_i), DC gain (K_i) and natural frequency (ω_{ni}).

The current version of the model outputs the Robot Velocity and Acceleration, both translational and orientational (Euler Rates and Angular Velocity), in relation to the inertial frame. This was implemented without any direct derivative computation. The model was adapted from the second order SLIT written to the Phase Variable, so that it outputs the speed and the acceleration in each channel directly.

The time-domain identification was performed by means of a Genetic Algorithm and the Interior Point algorithm, using a successive continuous steps signal. This signal evinces the dynamic characteristics, the time-transport delay, the moving average filter and the non-linearities (dynamic workspace limits) of the robot. It can drive the robot to a fail/stop getting it out of the dynamic workspace limit (stopping by excessive torque or presenting some jerk).

3.4 Selected Flight manoeuvres

Attempting to discriminate the characteristic motion of a helicopter, a set of discrete manoeuvres covering the different motion channels and

tilt coordinations were selected from the *ADS-33E* [24] standard. Unless specified, the current approach follows the work of Schroeder [4] where an extended methodology for helicopter flight simulation is elaborated.

3.4.1 Vertical motion

A bob-up manoeuvre is selected, being reported to represent a generic helicopter dynamics in vertical motion. The representing transfer function is

$$\frac{\ddot{h}}{\delta_c} = \frac{9s}{s + 0.3} \quad (5)$$

3.4.2 Roll-sway

Lateral motion model assumes that dynamic response to control inputs result in an isolated coordinated manoeuvre. The representative dynamics results in a sequence that is initiated by lateral roll-control input, leading to helicopter roll (ϕ), which in consequence drives the helicopter to translate laterally to a position y . Following [12] The the system is represented by:

$$H_\phi(s) = \frac{\phi(s)}{\delta(s)} = \frac{L_\delta}{s(s + L_p)} \quad (6a)$$

$$H_y(s) = \frac{y(s)}{\phi(s)} = \frac{g}{s^2} \quad (6b)$$

In both cases δ represents the roll angle ϕ control input, for the latter case, L_δ and L_p are the control gain and roll damping coefficient respectively. It is important to note that in the former case control input δ is normalized in a range from $[-1 : 1]$ and for the latter case δ is given in radians and $L_\delta = 5.1s^{-1}$ and $L_p = 4.5s^{-1}$.

3.4.3 Yaw

For yaw dynamics, two sub-cases are represented so isolated yaw can be simulated and coupled compensation (climb-yaw) can be studied. For isolated yaw the model used by Hodge et al. [11] will be used, thus yaw dynamics is given by

$$\frac{\ddot{\Psi}}{\delta_{ped}}(s) = \frac{N_\delta s}{s - N_r} \quad (7)$$

As reported, corresponding values for yaw damping derivative and pedal sensitivity are $N_r = -0.33sec^{-1}$ and $N_\delta = \pm 0.25rad/s^2$ and $\delta = \pm 2.25in$, thus mimicking the response of a UH-60 helicopter.

Pilot location with respect to rotation center of a given simulated helicopter are considered by including the offset effect on linear accelerations perceived by the pilot as follows

$$a_{x_p} = -x_{pos}\ddot{\Psi}^2 \quad (8a)$$

$$a_{y_p} = y_{pos}\ddot{\Psi} \quad (8b)$$

4 Washout Filter tuning

Filter tuning in this work is attempted through an optimization approach. The main idea behind it lays on the hypothesis that if the vestibular model is included, at least the motion cueing will drive the tuning of the different variables of the Washout filters. This, arguing that the final outcome of any flight simulator is to achieve, not only similar perception of events but also similar actions from the pilot while operating the system, mixing all the sensors, dynamic and simulating subsystems involved.

The optimization strategy then, looks to compare two similar systems. The first system is defined such that the pilot will be modelled along with the aircraft model but with no consideration of a motion platform, that is, the case is considered the nominal "in-flight" case. The second system will consider the washout filters and the platform motion within the loop, including the motion constraints and its representative dynamics, thus forcing the optimization to stay within the variable boundaries. With both, "nominal" and "simulated" systems defined, the simulated system will try to emulate the nominal one by aiming towards the minimization of a *Cumulative Root Mean Square* (CRMS) which compares the motion cues signals after being treated with the vestibular model present in each system.

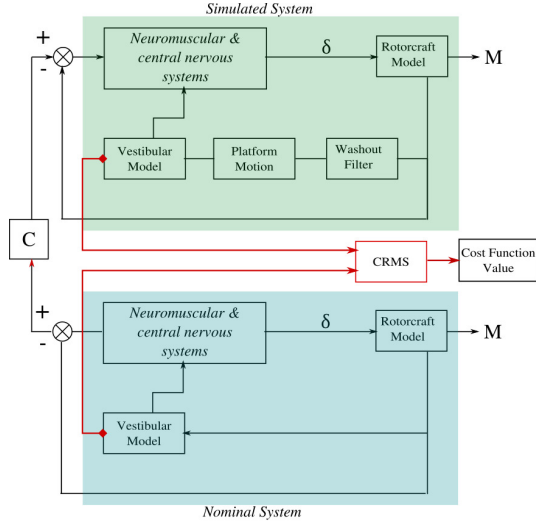


Fig. 4 Nominal and simulated systems for optimization

4.1 A case for validation

As an initial test, the bob-up case built by Schroeder [4] is replicated here in two different systems as explained before. Since the bob-up implies a vertical motion and isolates rotations or tilt coordination, only the Otolith model is included inside the Structural model, and the reported Vertical Motion Simulator (VMS) representative dynamics for the motion servo hardware is reported as

$$\frac{\ddot{h}_{sim}}{c\ddot{o}m}(s) = \frac{(8)(26)}{(s+8)(s+26)} \quad (9)$$

and the washout filter correspond to

$$\frac{\ddot{h}_c}{\ddot{h}}(s) = k \frac{s^2}{s^2 + 2\zeta\omega s + \omega^2} \quad (10)$$

for which \ddot{h}_c and \ddot{h} are the commanded and perceived vertical acceleration respectively. k is the motion gain while ω is the filter frequency and $\zeta = 0.7$ is the damping ratio, thus leaving the frequency and gain to be used as optimization parameters.

Variable settings and constraints were set as follows:

The vestibular model is saturated according to the human perception threshold such that angular

rates hold between $0.1^\circ/s - 0.5^\circ/s$. Initial settings for motion gain k and frequency ω are set to 0.010 and 1 respectively, thus using the same initial values of Schroeder for his zero order dynamics, i.e. no motion platform is considered. Their values are allowed to vary in the range of $[0 : 1]$ Tolerances for convergence are set as 10^{-5} for both, cost function value and parameter variation. Finally, platform motion is constrained to the reported physical limits of $\pm 9.14m$ ($\pm 30ft$).

Considering the relatively small space of search, optimization process is set to use a pattern search with a Latin hypercube.

Remembering that the main purpose is to best replicate both, perception and pilot actions, the cost function is defined as a Root Mean Square is used to compare the behaviour of the nominal system (with feedback directly from aircraft model) and simulated system (including the motion platform in the feedback rout to the pilot). Results for this case are shown in figures Fig. 5 and Fig. 6.

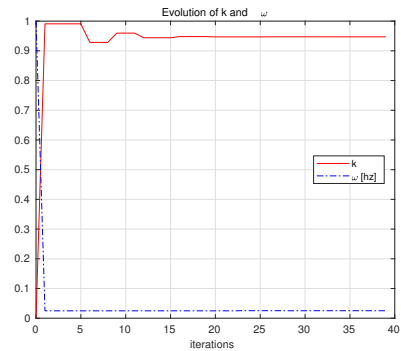


Fig. 5 Cost function and parameters evolution

As can be observed in Fig. 6, convergence is obtained for $k = 0.9471$ and $\omega = 0.0252$. For these values, perceived acceleration at pilot station, overall system response and collective control show good tracking compared to the nominal model. As a relevant point, the resulting values for the motion gain and frequency represent a close resemblance to those of Schroeder for the high fidelity simulation case, around $k = 0.901$ and $\omega = 0.245$ which are the next values in fidelity grade after the nominal behaviour i.e. $k =$

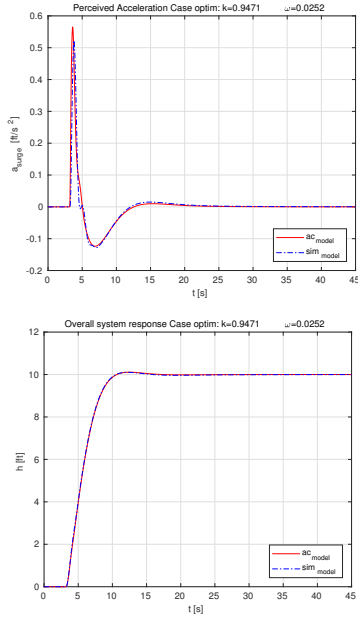


Fig. 6 Results for optimal case considering platform motion for $k = 0.9471$ and $\omega = 0.0252$

1.0 and $\omega = 0.0$.

4.2 The SIVOR case

In this section, results of optimization process is shown for the three aforementioned maneuvers. A complete set of washout filters was set, covering the XYZ positions and $\phi\theta\psi$ angles, this was done to provide freedom to the optimization routine hoping to capture the behavior of the system in regard to the isolation of the implemented discrete maneuvers. In every case, initial points for optimization were set as in the validation case and the same optimization method and tolerances were followed.

Fig. 7 shows the result for the bob-up case. For this case, the main difference is set by the vertical motion constraint of the robot, as opposite to the validation case where no scaling was needed due to the large vertical range of motion of the motion platform, SIVOR range is more limited ($\pm 1.5m$) and that constraint can be noticed leading the behavior of the perceived acceleration departing from the nominal

behavior. Nevertheless, the system behavior seems not to be affected by the mismatch in perceived acceleration, showing basically little or no difference with respect to the reference path, this considering that the SPM provides also a visual cueing supporting that of motion.

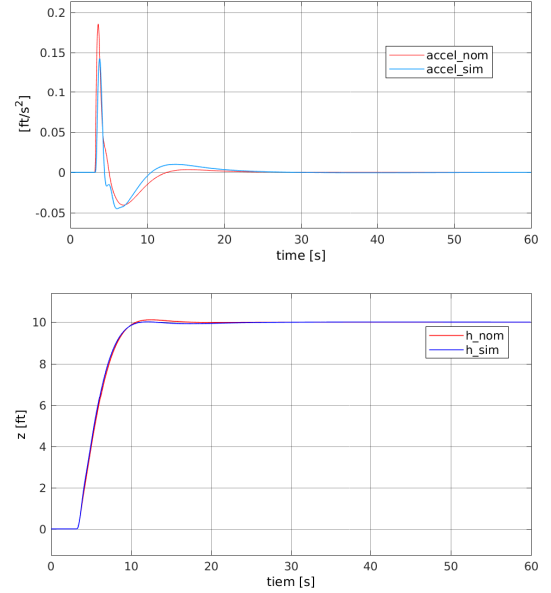


Fig. 7 Results for optimal filter parameters, Bob-up maneuver (top: perceived acceleration, bottom: system vertical response)

Fig. 8 shows the result for the roll-sway case. This result shows good agreement for the lateral acceleration perception (top) as well as for the roll angle ϕ (third from top) and Y_{pos} (bottom) behaviors, nevertheless, it clearly shows a disagreement for the rotational rate perception. This result was not necessarily surprising. The observed behavior shows that the overall system behavior can be achieved by a mixture of the more relevant lateral acceleration and the visual cueing in both, inner and outer loops. This is something that follows the findings of Hodge et.al. [12], where it was concluded that perceived fidelity improved from a well balanced combination of filter gains preferring a high sway gain and low roll gain, this also can be related with the constraints used for this work, limiting motions to 1.5m lead-

ing the system to behave as a short-stroke system, from which the cited findings were derived. An important observation is that there is little observed phase error in the results, suggesting that the maneuver in the simulation is well coordinated, something that, as has been reported in the literature, favours the perceived fidelity.

Yaw case behavior is shown in Fig. 9. The SPM setting of this maneuver included a threshold, limiting the x-axis accelerations to be larger than a minimum to avoid the generation of noise like behaviour on the surrogate visual cue. If the acceleration was below the threshold, then it was assumed that the pilot would resort to the visual cue in its totality. For this case, the system behaves well for lateral accelerations rates and yaw tracking, not doing so for the acceleration along the x-axis. This result though, seems to agree with published findings from Schroeder [4], where it was found that for the yaw case, lateral motion provided a better simulation fidelity and that rotational motion provided marginal improvements. Nevertheless, Hodge et.al. [11] also present a study on Yaw simulation, testing combinations for rotational+lateral motions while studying the pilot technique. In their findings, a combination of rotational and lateral motions would improve perceived fidelity. But the same study also calls for attention to the location of pilot with respect to axis of rotation in the simulated aircraft, mentioning that if the offset is large, then yaw motion would be below the perception threshold and the dominant motion would be the lateral one. Considering the 10 ft off-set used in the model for this case, the results seem to agree with that observation.

4.3 Conclusions

This work was intended as an initial exploration of the possibilities of an objective model-based to the flight simulation motion cueing problem.

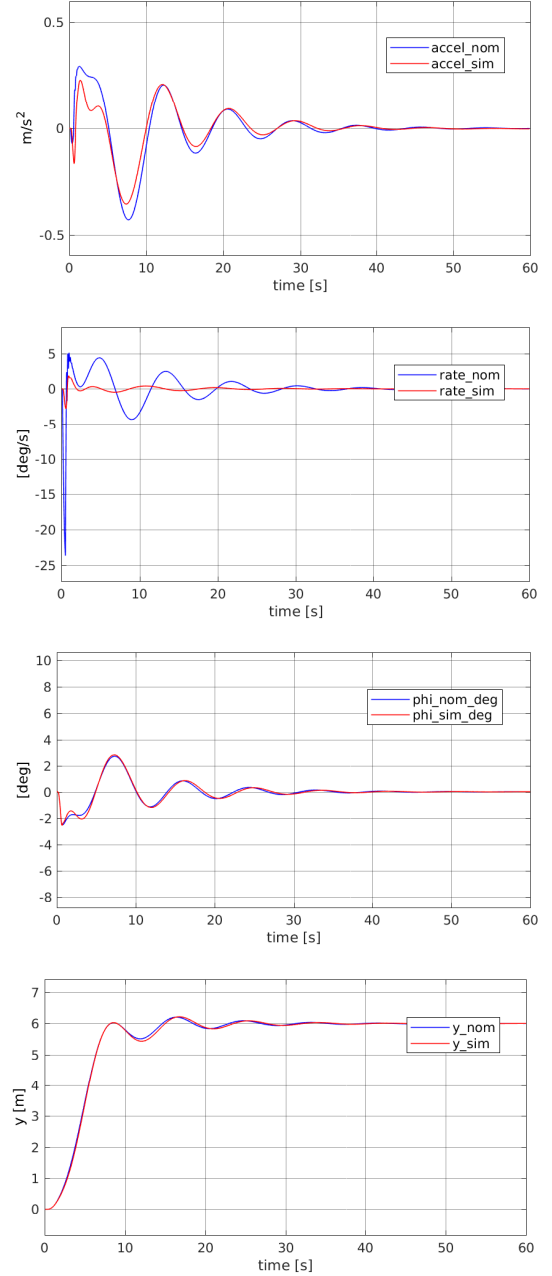


Fig. 8 Results for optimal filter parameters, Roll-sway maneuver (top to bottom: perc. acceleration, perc. angular rate, ϕ angle and lateral position y)

The SPM was modified to include the vestibular model in the inner loop and to provide a base grading in regard to fidelity. The identified robot model provided flexibility in regard to testing and the maneuvers provided discrimination of the relevant dynamics involved in each

case. Results seem to agree well with previous research and experimental results, it is hoped that this study will include experimental expansion in further work.

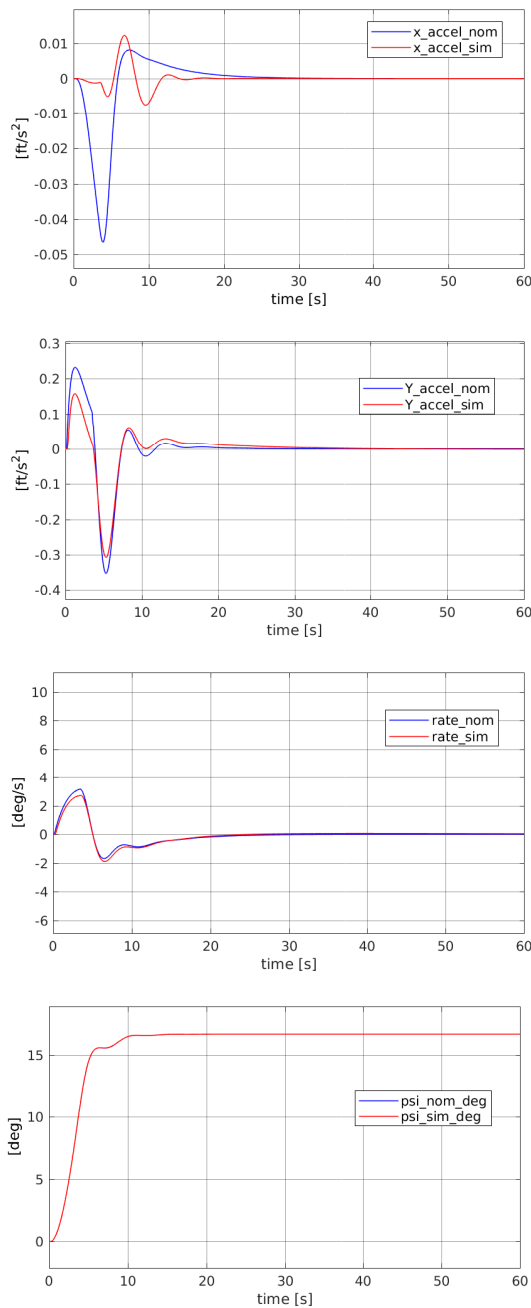


Fig. 9 Results for optimal filter parameters, Yaw maneuver (top to bottom: perc. X-acceleration, perc. Y-acceleration, perc. angular rate, and ψ angle)

5 Acknowledgements

The authors would like to thank Prof. Ronald Hess at University of California, Davis, for his kind advice during the development of this work. The first author also would like to acknowledge the kind and prompt cooperation received from the personnel of CCM laboratory at Instituto Tecnológico de Aeronáutica and to COLCIENCIAS for sponsoring the participation in the project.

References

- [1] Pavel MD, White MD, Padfield GD, Roth G, Hamers M, and Taghizad A. *Validation of mathematical models for helicopter flight simulators current and future challenges*, The Aeronautical Journal, RAeS, Volume 117, Number 1190, pp. 343-388. April 2013.
- [2] Padfield GD, Pavel MD, Casolaro D, Roth G, Hammers M and Taghizad A. *Validation criteria for helicopter real-time simulation models: Sketches from the work of Garteur HC-AG12*. Presented at the 30th European Rotorcraft Forum, Marseilles, France, Sept. 2004.
- [3] Perfect P, White M, Padfield G, Gubbels A, Berryman A. *Integrating predicted and perceived fidelity for flight simulators*. European Rotorcraft Forum 2010, Paper Number 061.
- [4] Schroeder J. *Helicopter flight simulation motion platform requirements*. NASA/TP-1999-208766. Ames Research Center, Moffet Field, Ca. 1999.
- [5] Gennaretti M, Prcacchia F, Migliore S. and Serafini J. *Assessment of Helicopter Pilot-in-the-loop Models*, Hindawi, International journal of Aerospace Engineering, 2017.
- [6] Grant P. and Reid L. *Motion Washout Filter Tuning: Rules and Requirements*, Journal of aircraft, Vol. 34, No.2, March-April 1997
- [7] Lone M, Cooke A. *Review of pilot models used in aircraft flight dynamics*, Elsevier, Journal of Aerospace Science and Technology Vol. 34 pp 55-74, 2014.
- [8] Perfect P., White M., Padfield G., Gubbels A. *Rotorcraft simulation fidelity: new methods for quantification and assessment*. The Aeronautical Journal, Vol. 117, No. 1188, February 2013.

- [9] Wiskemann C., Drop F., Pool D., van Paassen M., Mulder M., B  ijlthoff H. *Subjective and Objective Metrics for the Evaluation of Motion Cueing Fidelity for a Roll-Lateral Reposition Maneuver*. Presented at the AHS 70th Annual Forum, Montr  al, Quebec, 2014.
- [10] Nieuwenhuizen F. and B  ijlthoff H. *The MPI CyberMotion Simulator: A Novel Research Platform to Investigate Human Control Behavior* Journal of computing science and engineering, Vol. 7, No. 2, pp. 122-131 June 2013.
- [11] Hodge S., Perfect P, Padfield G, White M. *Optimising the yaw motion cues available from a short stroke hexapod motion platform*. The Aeronautical Journal, Vol. 119, No. 1211, pp. 1-21, January 2015.
- [12] Hodge S., Perfect P, Padfield G, White M. *Optimising the roll-sway motion cues available from a short stroke hexapod motion platform*. The Aeronautical Journal, Vol. 119, No. 1211, pp. 23-44, January 2015.
- [13] Hess R. *Unified Theory for Aircraft Handling Qualities and Adverse Aircraft-Pilot Coupling*. Journal of Guidance, Control and Dynamics. Vol. 20, No.6, pp. 1141-1148, November-December 1997.
- [14] Zeyada Y., Hess R. *A methodology for evaluating the fidelity of ground-based flight simulators*. Presented at the AIAA Modeling and Simulation Conference and Exhibit, Portland Oregon, 9-11 August 1999.
- [15] Hess R., Malsbury T., and Atencio A. *Flight simulator fidelity assessment in a rotorcraft lateral translation maneuver*. Journal of Guidance, Control and Dynamics. Vol. 16, No.1, pp. 79-85, January-February 1993.
- [16] Hess R. and Siwakosit W. *Assessment of Flight Simulator Fidelity in Multiaxis Tasks Including Visual Cue Quality*. Journal of Aircraft, Vol.38, No.4 pp. 607-6014, August 2001.
- [17] Hess R. and Malsbury. *Closed-loop assessment of flight simulator fidelity*. Journal of Guidance, Control and Dynamics. Vol. 14, No.1, pp. 191-197, January-February 1991.
- [18] Hess R., Zeyada Y. and Heffley R. *Modeling and Simulation for Helicopter Task Analysis*. Journal of the american helicopter society, Volume 47, Number 4, pp. 243-252, October 2002.
- [19] Fernandez C. and Goldberg P. *Physiology of peripheral neurons innervating semi-circular canals of the squirrel monkey II: Response to sinusoidal stimulation and dynamics of peripheral vestibular system*. Journal of Neurophysiology 34, pp. 661-675, 1971.
- [20] Reid L. and Nahon M. *Flight Simulation Motion-Base Drive Algorithms: Part 2 - Selecting the System Parameters*. Report 307, UTIAS. 1986.
- [21] Isermann R., M  ijnchhof M., 2011, *Identification of Dynamic Systems: An Introduction with Applications*. Springer, Berlin, 2011.
- [22] Teufel, H.J., Nusseck, H.G., Beykirch, K.A., Butler, J.S., Kerger, M., and B  ijlthoff, H.H. *MPI Motion Simulator: Development and Analysis of a Novel Motion Simulator*. AIAA Modeling and Simulation Technologies Conference and Exhibit, Vol. 1, AIAA, Hilton Head, South Carolina, pp. 1 - 11, 2007.
- [23] Craig, J. *Introduction to robotics: mechanics and control*. Transl. to Portuguese of Heloisa Coimbra de Souza, Tech. Revision of Reinaldo Augusto da Costa Bianchi, 3. ed. S  o Paulo, Pearson Education do Brasil, 2012.
- [24] Handling qualities Requirements for military rotorcraft. Aeronautical design standard 33D (ADS-33D), U.S. Army Aviation and Troop Command, St. Lois, Mo. July 1994.

6 Contact Author Email Address

Wesley Rodrigues de Oliveira
mailto: wesleyro@ccm-ita.org.br

Copyright Statement

The authors confirm that they, and/or their company or organization, hold copyright on all of the original material included in this paper. The authors also confirm that they have obtained permission, from the copyright holder of any third party material included in this paper, to publish it as part of their paper. The authors confirm that they give permission, or have obtained permission from the copyright holder of this paper, for the publication and distribution of this paper as part of the ICAS proceedings or as individual off-prints from the proceedings.